

Ferroelectric Nematic Liquid Crystal Electro-Optics

Noel A. Clark¹, Xi Chen¹, Joseph E. Maclennan¹, Matthew A. Glaser¹

noel.clark@colorado.edu

¹Department of Physics and Soft Materials Research Center, University of Colorado, Boulder, CO 80309, USA

Keywords: Ferroelectric nematic liquid crystal, Polar molecules, Electro-optics

ABSTRACT

Ferroelectric Nematic liquid crystals offer new opportunities for electro-optic science and applications, based on strong coupling of director orientation to applied electric field, afforded by spontaneous ferroelectric polarization. Here we discuss self-interaction and interfacial electrostatic effects that must be considered in order to develop attractive and useful ferroelectric nematic electro-optics.

1 Introduction

A novel nematic liquid crystal phase [1,2,3,4] has recently been shown to be a ferroelectric nematic (N_F) [5], offering opportunities for a variety of new LC field and surface phenomena. The ferroelectric nematic is a 3D liquid with a macroscopic electric polarization $\mathbf{P}(\mathbf{r})$ [5]. On the nanoscale, each molecular dipole is constrained to be nearly parallel to its molecular steric long axis, which translates macroscopically into a strong orientational coupling making $\mathbf{P}(\mathbf{r})$ locally parallel to $\pm\mathbf{n}(\mathbf{r})$, the local average molecular long axis orientation and uniaxial optic axis of the phase [5]. The polarization thus endows the N_F with coupling between $\mathbf{n}(\mathbf{r})$ and applied electric field, \mathbf{E} , that is linear and is dominant over the dielectric coupling at low E . The N_F phase exhibits self-stabilized, spontaneous polar ordering that is nearly complete [3,5], with a polar order parameter, $p = \langle \cos(\beta_i) \rangle \gtrsim 0.9$, where β_i is the angle between a typical molecular dipole and the local average polarization density \mathbf{P} . The resulting large spontaneous polarization ($P \sim 6 \mu\text{C}/\text{cm}^2$) enables field-induced nematic director reorientation and an associated electro-optic (EO) response with applied fields in typical cells as small as $\sim 1 \text{ V}/\text{cm}$, a thousand times smaller than those used to reorient dielectric nematics [6].

The strong polar nature of the NF also results in transformative novelty in the interaction of the LC with bounding surfaces, a key aspect of nematic LC science and its potential for technology [6]. Desired vectorial orientation distributions within a 3D volume of polar molecules can be achieved by controlling the polarity of its 2D bounding surfaces. In the simplest example, if the orientation of the preferred polarization is identical on the surfaces of the two parallel glass plates forming a cell, then the N_F volume polarization can be similarly oriented,

that is, poled into a uniform orientation by the surfaces, without the need for an applied field [6]. Alternatively, twisted director structures can be stabilized if the preferred surface orientations on opposite plates are anti-parallel [6].

While the potential for using such effects is exciting, the strong polar ordering of ferroelectric nematics also produces ubiquitous space charge and polarization self-interaction effects that may significantly alter their static and dynamic behavior [5,6]. We provide several examples in this presentation.

2 Electro-Optics and Dynamics

The field-induced orientational dynamic responses of N_F cells can be classified into two principal types, one characteristic of field rotation (ROT), occurring when a component of \mathbf{E} appears in the direction normal to \mathbf{P} , and the other typical of field reversal (REV), occurring when the component of \mathbf{E} parallel to \mathbf{P} changes sign. In the simplest case where the induced molecular reorientation $\varphi(x,t)$ varies in only one dimension, the bulk response to \mathbf{E} is governed by the dynamic torque balance equation, $T_E = \gamma \partial \varphi / \partial t = -PE \cos \varphi + K \partial^2 \varphi / \partial x^2$, where γ is the nematic rotational viscosity and K the Frank elastic constant.

In the ROT response regime, the torque applied by the field, $T_E = -PE \cos \varphi$, tends to rotate \mathbf{P} toward the field direction, $\varphi = 90^\circ$. Each element of the cell is effectively elastically decoupled from its neighbors, reorienting independently in the applied field. The polarization responds in a continuous fashion without altering the topology, except for surface regions where the surface preferred orientation is squeezed into a thickness comparable to the deGennes field penetration length $\xi_E = \sqrt{(K/PE)}$. ξ_E is small in N_F phases with large polarization ($\xi_E \sim 50 \text{ nm}$ for $P = 6 \mu\text{C}/\text{cm}^2$ and an applied field $E = 40 \text{ V}/\text{mm}$ [5]).

A simple ROT application of the torque balance equation is calculation of the static and dynamic splay-bend director deformation response of an N_F, initially with a uniform director and polarization in the planar aligned sandwich cell geometry, shown in Figs. 1 and 2. The field is applied normal to the cell plates with ITO electrodes coated with buffed polyimide alignment layers,

and a 4.5 μm thick LC layer, viewed in transmission between crossed polarizer and analyzer. The sample temperature is held near the N–N_F transition, a small, in-plane temperature gradient ensuring that part of the sample is in the N_F phase while the rest is in the N phase, with a wide transition region (demarcated by white and black dashed lines in Fig. 1) where the two phases form overlapping wedges. Applying triangle waves from 1 Hz (slowly varying DC) to 1 kHz of varying peak amplitude in the range ($0\text{V} < V_p < 5\text{V}$) can induce the Freedericksz transition in the N phase, substantially reducing its birefringence, but gives no significant detectable response in the N_F, as shown in Fig. 1, in spite of the optimal geometry for the coupling of \mathbf{P} and \mathbf{E} , maximizing \mathcal{T}_E . This apparent lack of response is an example of “polarization self-interaction”, discussed next, an array of phenomena arising from polarization-generated space charge and its long-ranged electrostatic interaction.

3 Polarization Self-Interaction (PSI)

Spatial variation of $\mathbf{P}(\mathbf{r})$ generally results in bulk and surface polarization charge density, given respectively by $\rho_P = \nabla \cdot \mathbf{P}(\mathbf{r})$ and $\sigma_P = \mathbf{P}_s \cdot \mathbf{s}$. The electric field generated by the bulk charge opposes the bulk distortion of $\mathbf{P}(\mathbf{r})$ that caused it, producing a bulk energy $U_P = \frac{1}{2} [dV \nabla \cdot \mathbf{P}(\mathbf{r}) \nabla \cdot \mathbf{P}(\mathbf{r}')] \{1 / |\mathbf{r} - \mathbf{r}'|\}$ [7-13]. Assuming, with \mathbf{P} along x , a periodic transverse modulation $\delta P_y(\mathbf{r})$ of amplitude $P \delta n_y$ and wavevector q_y , so that $\nabla \cdot \mathbf{P}(\mathbf{r}) = \partial P_y(y) / \partial y = i q_y P \delta n_y$, we have an elastic energy density $U_{sp} = \frac{1}{2} [K_s q_y^2 + 4\pi P^2 / \epsilon] |\delta n_y|^2$, meaning that the polarization term will be dominant for $q_y < \pi \sqrt{2} / \xi_P$, where $\xi_P = \sqrt{\epsilon K / P^2}$ is the polarization self-penetration length. Since for $P = 6 \mu\text{C}/\text{cm}^2$ we have $\xi_P \sim 0.1 \text{ nm}$, this dominance, if not screened, will act down to molecular length scales at which other effects such as N_F phase stability, will likely come into play. The result is that the polarization field tends to be spatially homogeneous, with electric field-induced reorientations occurring via blocks of uniform orientation free of splay. Then low-energy elastic distortions of the \mathbf{n}, \mathbf{P} couple allow only bend, with splay of $\mathbf{n}(\mathbf{r})$ and $\mathbf{P}(\mathbf{r})$ expelled from the bulk and confined to reorientation walls. An example of this is shown in Fig. 3.

All such polarization-based effects are reduced by free space charge, such as ionic impurities in the LC and its containing surfaces [9], ionization of the LC itself, and charge injected from the electrodes, all of which tend to screen the polarization charge. In SmC* (FLC) cells, when the P is small ($P < 20 \text{ nC}/\text{cm}^2$) the bound polarization charge can be substantially screened but for large polarizations ($P > 100 \text{ nC}/\text{cm}^2$) the free charge supply can be exhausted and polarization effects manifested. For the largest SmC* polarizations ($P \sim 800 \text{ nC}/\text{cm}^2$), the polarization charge is largely unscreened and the polarization effects are quite dramatic [13]. Thus, the SmC*

FLC literature provides examples of screened and unscreened FLC behavior from which we can infer that the polarization charge of the N_F phase is largely unscreened by ions. The DC conductivity of our RM734 sample is $\sigma \sim 10^{-7} (\text{Ohm}\cdot\text{cm})^{-1}$, which is small enough to contribute little to the measurement of P and not affect the N-phase Freedericksz transition, but large compared to typical 5CB for example, which is $\sigma \sim 10^{-10} (\text{Ohm}\cdot\text{cm})^{-1}$. Estimating the Debye length λ_D using the ion density from σ gives $\lambda_D \sim 1\text{mm}$, consistent with the observation that applied in-plane fields appear to be generally uniform and unscreened over millimeter dimension areas as in Fig. 3, so the Debye length must be this size or larger.

3.1 PSI Example: "Block Polarization" Reorientation

The behavior in Fig. 1 can be understood on the basis of the "block polarization" model developed to explain V-shaped switching in high-polarization FLCs [8,9], and shown schematically in Fig. 2. In this model, polarization charge induced by reorientation of \mathbf{P} completely cancels \mathbf{E} in the LC and the polarization direction is electrostatically controlled by this condition. Insulating layers without reorienting polarization at the LC/glass interfaces such as the polymer alignment layer, charge depletion in the ITO, and bound polarization at the surface, are accounted for as capacitive elements with a net capacitance per unit area, C . With these assumptions, the orientation of the polarization field as a function of applied voltage V is given by $\sin\phi(V) = V/V_{\text{sat}}$, where $V_{\text{sat}} = 2P/C$, [10,11,13], showing that when P is large, a large applied voltage is required to achieve substantial reorientation of \mathbf{n}, \mathbf{P} . This N_F cell can be compared with the bent-core SmAP_F ITO electro-optic FLC cell of Ref [13], where a saturation voltage $V_{\text{sat}} = 15 \text{ V}$ was measured for material with $P = 0.85 \mu\text{C}/\text{cm}^2$, leading us to expect $V_{\text{sat}} \sim 100 \text{ V}$ for LC in the N_F phase with $P \sim 6 \mu\text{C}/\text{cm}^2$ in a cell with 50 nm-thick insulating layers with $\epsilon = 5$ at the two cell boundaries. It is therefore not surprising that the N_F phase shows little response in the applied voltage range explored here: only a tiny reorientation of \mathbf{P} generates enough charge to cancel the field from the free charge.

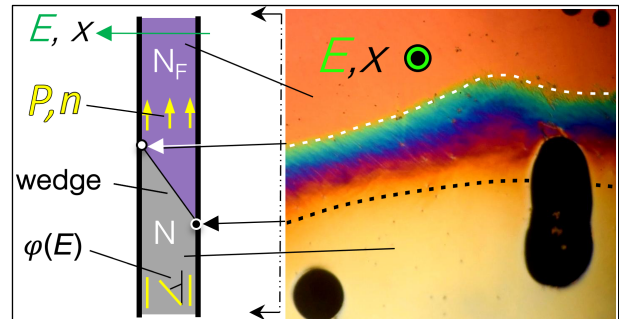


Fig. 1: Sandwich cell with N and N_F phase areas.

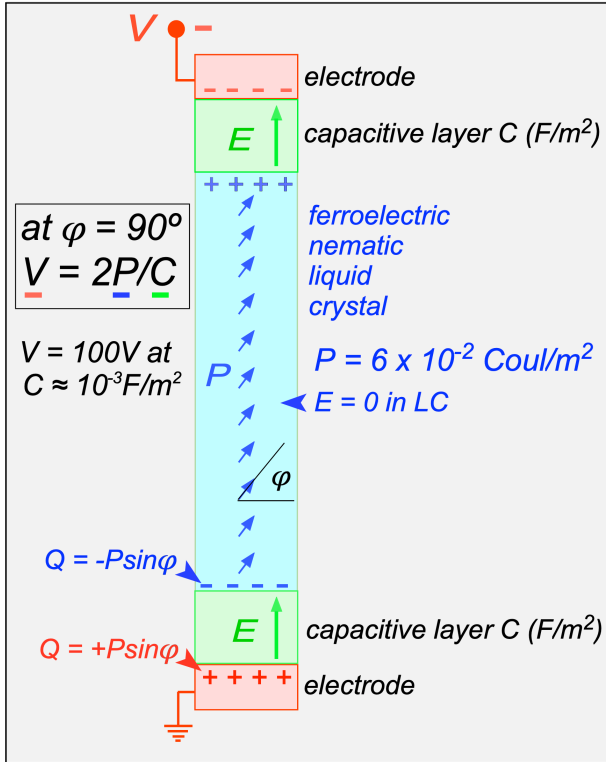


Fig. 2: Sandwich cell block polarization geometry.

While the large value of P ensures a strong coupling of orientation to applied field, it also produces ubiquitous space charge effects that may significantly alter the dynamics. In cells with in-plane electrodes studied here, there is an effective thin, insulating barrier at the interface between the N_F phase and the electrodes, a barrier which either has no polarization or in which the polarization is fixed in orientation. Such layers drop part of the applied voltage in maintaining the physical separation of free charge carriers from the polarization charge accumulated at the insulating interface with the ferroelectric LC. Such a layer is formed, for example, by the polymer films used for alignment but even in cells where there is no alignment layer and the interface is N_F /gold, the cell behavior indicates that such an insulating layer exists. If this layer has a capacitance C Farads/cm², then the effective field in the above equation for $\varphi_E(t)$ is reduced by the depolarization voltage $(P/C)\sin\varphi_E(t)$, becoming $E = [V_{IN} - (P/C)\cos\varphi_E(t)]/L$. Generally, these interfacial layers are not perfectly insulating, with free charge passing through to the polarization charge layer, in which case they can be modeled as a material of resistance $R \Omega\text{-cm}^2$ in parallel with C (a leaky capacitor).

3.2 PSI Example: Field-Induced Bend Wave

Fig. 3 shows the response of a uniformly planar-aligned N_F region in a 4.5 μm thick RM734 cell to an increasing in-plane DC field in the range $0 < E < 2$ V/cm that initially opposes the local polarization. The response is to form a bend wave in the n - P field, zig-zag modulation in the

orientation of $n(r)$ and $P(r)$ in which the non-zero spatial variation is $\partial n(r)/\partial x$, along the director, making it a bend wave. Green vectors indicate field-induced reorientations. Bend has a lower polarization space charge energy cost than a splay wave (nonzero $\partial n(r)/\partial y$, which would generate stripes parallel to n rather than normal to it). As the field strength is increased, the degree of reorientation increases and distinct boundaries appear between the half-periods of the modulation, separating stripes of uniform internal orientation. Fields of a few V/cm drive complete $(+\pi, -\pi, +\pi, -\pi)$ reorientation of n , for which these boundaries become 2π walls, sub-optical resolution ($\sim \xi_P$) in width. The zig-zag pattern of the stripes indicates an overall structure where P_z is constant, ensuring that there is minimal net polarization charge at the stripe boundaries, and where the backflow induced in each stripe matches that of its neighbor. The field is not strong enough to reverse the surfaces in this case. The herringbone arrangement of the director in the stripes ensures that the normal component of P is constant across the stripe boundaries, so that there is no net polarization charge on them. The zig-zag pattern also serves to reduce the transverse field E_y , generating alternating + and - charge on the region's upper and lower edges (white charges), instead of uniform charge density, which would fill the entire area with nonzero E_y . The zig-zag domain boundaries in (D) are 2π walls stabilized by pairs of oppositely charged sheets of splay-generated polarization charge. Solution of the static field equation $\mathcal{T}_E = 0 = -P(E_a + E_p)\sin\varphi + K\partial^2\varphi/\partial x^2$, where E_a is the applied field along x , and E_p is the field due to the polarization charge, given in Fig. 3, shows that these 2π walls are stable at $E_a = 0$ [12], with a structure of width $\Delta x \sim \xi_P$ given by $\cot[\varphi(x)/2] = -x/\xi_P$.

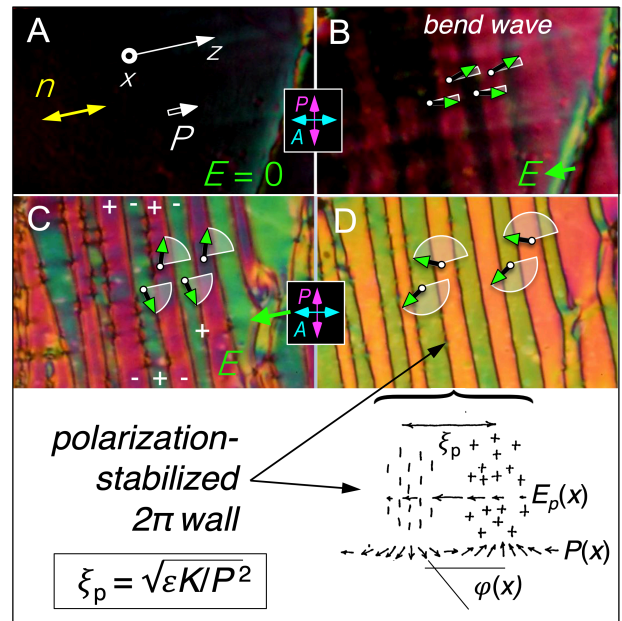


Fig. 3: planar cell block polarization geometry.

In the example of Fig. 3 the N_F LC layer is $4.5\mu\text{m}$ thick and the in-plane field provided by ITO electrodes on one of the glass cell plates, separated by a gap of 1mm . The potential difference required across the electrodes is small, only a few Volts. As is the sandwich cell geometry, capacitive insulating layers are formed on the electrodes, and polarization charge on their surfaces will reduce the electric field on the bulk LC, as for the sandwich case, especially at the electrode edges where the field is the largest. However, in contrast with the latter, the free charge on the electrode edges contribute only a small part of the field in the center of the electrode gap, so the latter can remain largely unscreened. If the area to be switched is limited in the y direction, e.g., pixelated, then in an induced reorientation, the polarization charge separating in the direction normal to the field (Fig. 3, white charges) can have a substantial retarding effect on field-induced reorientation and must be compensated with side electrodes.

4 Summary

These results show that the dipole distribution will organize itself to eliminate the electric field due to the polarization charge in all regions of space, save for sheets of width ξ_P as required by the boundary conditions. Thus if ξ_P is large compared to the LC cell thickness d , then the polarization space charge only weakly influences the n-P structure. On the other hand, for $\xi_P < d$, polarization charged disclinations will form at the cell interfaces. This basic result is an effective guiding principle in understanding the effect of polarization charge in ferroelectric LC cells,

5 Acknowledgements

This work was supported by NSF Condensed Matter Physics Grants DMR 1710711 and DMR 2005170, and by Materials Research Science and Engineering Center (MRSEC) Grant DMR 1420736.

References

- [1] R. J. Mandle, S. J. Cowling, and J. W. Goodby, "A nematic to nematic transformation exhibited by a rod-like liquid crystal". *Phys. Chem. Chem. Phys.* **19**, 11429-11435 (2017).
- [2] A. Mertelj, L. Cmok, N. Sebastián, R. J. Mandle, R. R. Parker, A. C. Whitwood, J. W. Goodby, M. Čopič, "Splay nematic phase". *Phys. Rev. X* **8**, 041025 (2018).
- [3] H. Nishikawa, K. Shiroshita, H. Higuchi, Y. Okumura, Y. Haseba, S. Yamamoto, K. Sago, H. Kikuchi, "A fluid liquid-crystal material with highly polar order". *Adv. Mater.* **29**, 1702354 (2017).
- [4] N. Sebastian, L. Cmok, R. J. Mandle, M. Rosario de la Fuente, I. Drevenšek Olenik, M. Čopič, A. Mertelj, "Ferroelectric-ferroelastic phase transition in a nematic liquid crystal". *Phys. Rev. Lett.* **124**, 037801 (2020).
- [5] X. Chen, E. Korblova, D. Dong, X. Wei, R. Shao, L. Radzihovsky, M. Glaser, J. Maclennan, D. Bedrov, D. Walba, N.A. Clark, "First-principles experimental demonstration of ferroelectricity in a thermotropic nematic liquid crystal: spontaneous polar domains and striking electro-optics". *Proceedings of the National Academy of Sciences of the United States of America* **117**, 14021-14031 (2020).
- [6] X. Chen, E. Korblova, M. A. Glaser, J. E. Maclennan, D. M. Walba, N. A. Clark, "Polar in-plane surface orientation of a ferroelectric nematic liquid crystal: polar monodomains and twisted state electro-optics". *Proceedings of the National Academy of Sciences of the United States of America* **118** (22), e2104092118 (2021).
- [7] R. B. Meyer, L. Liébert, L. Strzelecki, P. Keller, Ferroelectric Liquid Crystals.' *J. Phys.* **36**, L-69 (1975).
- [8] C. Y. Young, R. Pindak, N. A. Clark, R. B. Meyer, "Light-Scattering Study of Two-Dimensional Molecular-Orientation Fluctuations in a Freely Suspended Ferroelectric Liquid-Crystal Film." *Phys. Rev. Lett.* **40**, 773 (1978).
- [9] M. H. Lu, K. A. Crandall, C. Rosenblatt, R. G. Petschek, "Ion-Director Coupling in a Ferroelectric Liquid-Crystal." *Physical Review E* **47**, 1139-1143 (1993).
- [10] N. A. Clark, D. Coleman, J. E. Maclennan, "Electrostatics and the Electro-Optic Behavior of Chiral Smectics C: 'Block' Polarization Screening of Applied Voltage and 'V-Shaped' Switching. *Liquid Crystals* **27**, 985-990 (2000).
- [11] D. Coleman, D. Mueller, N. A. Clark, J. E. Maclennan, R. F. Shao, S. Bardou, D. M. Walba, "Control Of Molecular Orientation In Electrostatically Stabilized Ferroelectric Liquid Crystals." *Physical Review Letters* **91**, 175505 (2003).
- [12] Z. Zhuang, J.E. Maclennan, N.A. Clark, Device Applications Of Ferroelectric Liquid Crystals: Importance of Polarization Charge Interactions. *Proceedings of the Society of Photo-Optical Instrumentation Engineers* **1080**, 110-114 (1989).
- [13] Y. Shen, T. Gong, R. Shao, E. Korblova, J. E. Maclennan, D. M. Walba, N. A. Clark, "Effective Conductivity Due to Continuous Polarization Reorientation in Fluid Ferroelectrics." *Physical Review E* **84**, 020701(R) (2011).